

**EFFECT OF STRUCTURAL IMPERFECTIONS ON THE CHARACTERISTICS
OF YSZ DIELECTRIC LAYERS GROWN BY E-BEAM EVAPORATION
FROM THE CRYSTALLINE TARGETS¹**

**M. Hartmanová^{a,2}, M. Jergel^{a,b}, V. Navrátil^c, K. Navrátil^d, K. Gmucová^a,
F.C. Gandarilla^e, J. Zemek^f, Š. Chromik^g, F. Kundracik^h**

^a Institute of Physics, Slovak Academy of Science, SK-845 11 Bratislava, Slovakia

^b Departamento de Física, CINVESTAV – IPN, Apdo. Postal 14-740,
Mexico 07300, D.F., Mexico,

^c Department of Physics, Faculty of Education, Masaryk University,
60300 Brno, Czech Republic

^d Institute of Condensed Matter, Faculty of Sciences, Masaryk University,
61137 Brno, Czech Republic

^e Departamento de Ciencia de Materiales, Instituto Politecnico Nacional, U.P. ALM Lindavista,
Mexico 07738, D.F., Mexico

^f Institute of Physics, Academy of Sciences of the Czech Republic,
18 121 Prague 8, Czech Republic

^g Institute of Electrical Engineering, Slovak Academy of Sciences,
SK-841 04 Bratislava, Slovakia

^h Department of Experimental Physics, Faculty of Mathematics, Physics and Informatics,
Comenius University, SK-842 48 Bratislava, Slovakia

Received 7 January 2005, accepted 21 March 2005

The films under study were deposited by e-beam evaporation of yttria-stabilized zirconia (YSZ) crystalline samples on the n-doped Si (111) substrate at 750 °C. The XRD patterns of the films revealed their polycrystalline structure with a mixture of different phases, mainly the face-centered cubic one. The electrical conductivity and the activation energy as the functions of the yttria content indicated the influence of isolated oxygen ion vacancies as well as the associated point defects. The relative permittivities ($\epsilon_r = 17 - 26$) measured at room temperature and 1MHz confirmed YSZ as a high-k gate dielectric also in the form of thin film. The measured microhardness data, evaluated according to Jonsson-Hogmark composite hardness model, ($H = 5.9 - 10.8$ GPa), as well as a high refractive index ($n = 1.96 - 2.20$) render from YSZ a promising material for protective coatings and optical applications, respectively.

PACS: 82.45.Gj, 61.10.Nz, 66.30.Hs, 68.60.Bs, 78.20.-e

¹Presented at SSSI-IV (Solid State Surfaces and Interfaces IV) Conference, Smolenice, Slovakia, 8–11 Nov. 2004.

²E-mail address: maria.hartmanova@savba.sk

1 Introduction

Zirconia is one of the best examples of materials science where structure, microstructure, defects and phase composition / transformations are intimately connected with the macroscopic properties such as, for instance, electrical conductivity and microhardness. Thin films of zirconia have various applications in many important fields of interest ranging from solid oxide fuel cells (e.g. [1]), through the sensors (e.g. [2]), electrochemical devices (e.g. [3]), membrane reactors (e.g. [4]) up to protective coatings (e.g. [5]), microelectronics elements (e.g. [6]), etc. Such variety of applications stems from the polymorphism of zirconia, namely the existence of three different crystall phases: monoclinic (m), tetragonal (t) and cubic (c). The high temperature phases, (t) and (c), can be stabilized down to room temperature (RT) by an addition of aliovalent oxides as e. g. Y_2O_3 , CaO, MgO, etc.

The purpose of the present study was to continue in our investigation of zirconia polymorphism [7] with the aim to obtain a better understanding of the correlation between the crystallographic properties of YSZ thin films deposited from YSZ crystalline targets with well defined phase compositions and their optical, electrical and mechanical properties.

2 Experimental Details

Preparation of samples. Ytria stabilized zirconia (YSZ) films were deposited on n-doped Si (111) substrates by electron beam evaporation of $ZrO_{2+x} \cdot Y_2O_3$ ($x = 1.25, 3.24, 4.31$ and 9.21 mol%) crystalline samples used as targets. The temperature of deposition was $750^\circ C$. The details of the deposition can be found elsewhere [8].

The amount of yttrium ions in the deposited films was estimated by X-ray photoelectron spectroscopy (XPS). The measurements have been carried out in the ADES-400 (VG Scientific, UK) spectrometer equipped with a hemispherical angle resolved energy analyzer and an X-ray tube. The hemispherical energy analyzer was operated at a pass energy of 100 eV and at an emission angle of 90 deg with respect to the surface. The acceptance angle of the analyzer was set to be ± 4.1 deg. Photoelectron spectra were recorded using AlK α radiation (1486.6 eV, 300 W, angle of incidence 30 deg). The wide-scan spectra and narrow-scan spectra of the major constituents were recorded from each sample surface. Specially, the Y 3d and Zr 3d spectra were used to determine their atomic concentration ratios. The sample surfaces were analyzed without sputter-cleaning. The atomic concentrations were determined from the photoelectron peak areas corrected for the inelastic electron background, photoelectron cross-section [9], the inelastic mean free paths [10] and the experimentally determined transmission function of the hemispherical energy analyzer [11]. The atomic concentration ratios Zr/Y obtained together with the mol% Y_2O_3 calculated from these ratios and stoichiometry, can be seen in Table 1. The lower values of yttria amounts estimated in the deposited films than in the crystalline targets can be attributed to a higher volatility of yttria during the deposition process. The melting points of ZrO_2 and Y_2O_3 are $2663^\circ C$ and $2435^\circ C$, respectively (e.g. [12]). In order to obtain the equilibrium partial pressure 1×10^{-3} Torr, Zr and Y must be heated to the temperatures $2200^\circ C$ and $1500^\circ C$, respectively (e. g. [13]). It means that yttrium is more volatile than zirconium and the same situation can be expected for their oxides. Consequently, the yttria amounts in the deposited films are lower than in the crystalline targets. The film thicknesses, estimated by the surface profilometry using Talystep,

Tab. 1. Concentration (x) of Y_2O_3 in the YSZ thin films and the corresponding crystalline samples [7], atomic concentration ratio (Zr/Y) and thickness t of the thin films

x_{cryst} [mol% Y_2O_3]	$(Zr/Y)_{film}$	x_{film} [mol% Y_2O_3]	t_{film} [nm]
1.25	26.5	1.22	304
3.24	13.1	2.39	204
4.31	8.1	3.73	103
9.21	4.3	6.49	116

are also shown in Table 1. The reflectance measurements provided similar values, estimated with an accuracy of $\pm 0.2 - 0.3$ nm.

X-ray diffraction (XRD) measurements were performed in the surface sensitive grazing incidence geometry on a 12 kW Rigaku rotating anode generator at the angles of incidence fixed at 0.5° , 1.0° and 1.5° using CuK_α radiation. The dedicated laboratory-made diffractometer with a graphite monochromator in the primary beam was used. The 120° curved position sensitive INEL detector allowed a fast data collection.

A.c. conductivity measurements were done using a Solartron SI 1260 impedance / gain phase analyzer, interfaced to a computer and run through a Lab-view program. The impedance measurements were performed in the frequency range of 10 Hz – 1 MHz at temperatures RT – 753 K in air. The cell constant of deposited films reads $K = t/S$, S and t being the surface and film thickness, respectively. All electrical measurements were done in the metal-insulator-semiconductor (MIS) configuration with aluminium and gold as the top and bottom electrode, respectively. The top contact was evaporated through a metal mask to produce the circular gates of $0.886 \times 10^{-6} m^2$ area. The ohmic contact on the back side of the Si substrate was obtained by depositing of Au film.

Vickers microhardness measurements were done in air at room temperature (RT) by means of a Hanneman (Vickers) microhardness tester along with a Zeiss-Neophot microscope. Specimen indentations were performed with the load of 1.1 N (the test measurements of microhardness at three various loads 0.7, 0.9 and 1.1 N have shown the microhardness H to be independent on the load in this region). Three impressions were made under this load and both diagonals of each impression were measured 10-times. The average value obtained was used for the calculation (Sec. 3. 3., Eqn. (1)).

Reflectance measurements were carried out by the reflectance spectrophotometry using a double-beam spectrophotometer Varian CARY5E in the spectral region of 200 – 800 nm in air at room temperature. The measurements were performed by means of a circular light trace with a diameter of 2×10^{-3} m. The reflectance spectra were measured using a polished plate made from the crystalline silicon as a reflectance standard. The spectral dependence of silicon reflectance is well known (e.g. [14]). The maximum error of the reflectance measurements was ± 0.003 .

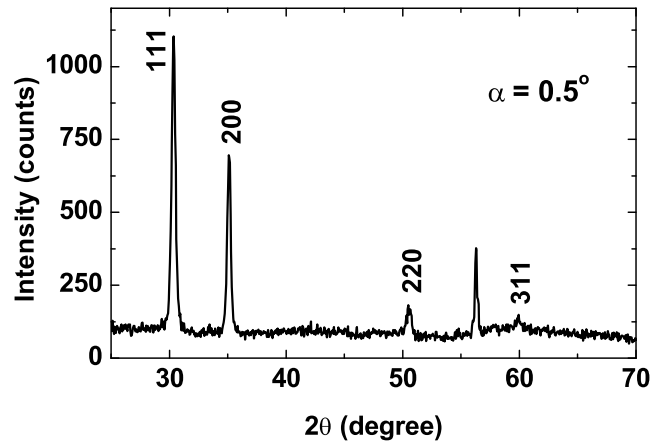


Fig. 1. Grazing incidence diffraction pattern of the film with 6.49 mol% Y_2O_3 measured at the angle of incidence 0.5° . The indices refer to the face-centered cubic phase.

3 Results and Discussion

3.1 Phase composition and structural parameters

In the first step, a general Rietveld analysis of the XRD patterns was performed and the presence of a face centered cubic (fcc) phase (space group $\text{Fm}\bar{3}\text{m}$) was found in the samples with 3.73 and 6.49 mol% Y_2O_3 , respectively. No satisfactory phase identification could be done in the samples with 1.22 and 2.39 mol% Y_2O_3 , however, it can be generally stated that the structure of the films under investigation is polycrystalline. An example of the diffraction pattern is shown in Fig. 1.

There is one unidentified peak, which is also the case of other samples, however, the unidentified peaks occur at different angles in different samples. From the relative fcc peak intensities, a tendency to one axial texture with (100) planes oriented preferentially parallel to the substrate can be concluded, the most obvious example being the sample with 3.73 mol% Y_2O_3 . Therefore in the second step, the Rietveld refinement was performed taking into account this texture, however, the fit quality was poor and prevented us from a reliable determination of the cell parameters and their correlation with the film composition. The perfection of the fcc phase in terms of Rietveld fitting decreases generally with the Y_2O_3 content.

Taking into account the experimental resolution, the crystallite size of the fcc phase fraction was determined from the integral width of 111 and 200 diffraction peaks. The effect of random lattice distortions (microstrain) on the peak broadening could not be included as a reliable, separation of the two effects can only be done for well developed and numerous peaks which is not our case. The crystallite sizes obtained in this way are 20.3 nm and 18 nm for the samples with

6.49 mol% Y_2O_3 and 3.73 mol% Y_2O_3 , respectively.

We tried to analyze also the unidentified peaks, either separately in each sample or putting them together into one “virtual” diffraction pattern. However, Hanawalt search [15] did not provide any satisfactory known phase. Therefore we may conclude only that the structure of all oxide film configurations was found to be polycrystalline and that the films contain at least two structurally different phases, one fcc with an increasing degree of perfection as Y_2O_3 content increases, and the other one which may be presumably a highly distorted form of some regular phase.

These structures of deposited YSZ films, not sufficiently developed during their growth, influence some investigated physical properties, mainly the electrical transport.

3.2 Electrical and dielectric properties

In the present study, our attention is paid to the frequency and temperature dependences of a.c. electrical conductivity as well as to the dielectric permittivities, the value of which is important for many applications.

It is well known that the structure-conductivity relationship is strongly dependent on the phase composition and structural parameters for the fluorite-related structures, what is our case. In the present study, a phase mixture with one relatively well defined cubic phase is observed in the two films with the highest yttria concentrations. The effect of yttria content and phase composition on both the electrical conductivity σ_b and the activation energy E_a is documented in Figs. 2 a, b. An example of impedance diagram is shown in the inset of Fig. 2 a. Two semicircles can be resolved in the impedance diagrams for all thin films investigated. The high-frequency one (≥ 200 kHz), can be attributed to the bulk. The relative permittivities ϵ_r calculated from this semicircle in the next paragraph are in a good agreement with those obtained by the other independent methods. The low-frequency semicircle (10 Hz – 30 kHz) was observable only at the higher temperatures with the equivalent resistance surpassing that of the bulk. The physical mechanism responsible for this semicircle cannot be determined unambiguously from the measured data. The origin could be crystallite boundaries, the presence of a thin (~ 1 nm) SiO_2 interlayer or small isolated SiO_2 islands on the surface of Si substrate leading to an imperfect electrical contact [16, 17, 18]. A combined effect of all these factors is possible too. The impedance diagram at the highest frequencies (the inset in Fig. 2 a) is slightly influenced by the presence of a parasitic inductance.

The bulk conductivity increases from 1.22 mol% Y_2O_3 to a maximum at 2.39 mol% Y_2O_3 , presumably due to an increase of the fraction of the more conductive phase. Further increase of the yttria content from 3.73 mol% Y_2O_3 to 6.49 mol% Y_2O_3 , results in the conductivity decrease. This decrease can be attributed to a decrease of the free oxygen vacancy concentration in the anion sublattice $Y_xZr_{1-x}O_{2-x/2}$ of solid solution induced by stronger interactions between the dopant cations and vacancies at low temperatures [7]. This fact indicates the influence of the isolated oxygen vacancies, $V_{\ddot{O}}$, which control the bulk ionic conductivity of the lightly doped samples and are generated by the presence of the substitutional Y^{3+} ions, as well as the associated point defects ($Y'_{Zr}V_{\ddot{O}}$). The formation of associated point defects (defect complexes) can be realized when the concentration of point defects increases. As it can be seen in Figs. 2 a, b, the concentration of oxygen vacancies is not large enough for the concentration of associated point defects to be significant for lower amounts of yttria approaching 1.22 mol% Y_2O_3 .

In general, the number of associated point defects increases with increasing amount of dopant. The associated point defects ($Y'_{Zr}V_{O}^{\bullet}$) control the low temperature transport properties of the samples with the highest concentrations of yttria. The calculated activation energy E_a exhibits a tendency to decrease with an increasing amount of yttria (Fig. 2 b), the minimum of E_a being observed at 2.39 mol% Y_2O_3 . The unusually low activation energy E_a , 0.15 – 0.49 eV, observed for the low-temperature conductivity of films is not well understood yet.

As it was mentioned above, the imperfections of the electrical contact in the films with the thickness ~ 100 nm, including the shorts through pinholes (microshort circuits), can influence the magnitude of the measured ohmic resistance and the shape of the impedance diagram. In the present study, the films thicknesses of 116 – 304 nm, are indeed very close to this approximate boundary of ~ 100 nm. However, the values of the effective relative dielectric permittivity ϵ_r , determined from the bulk semicircles of the impedance diagrams are in a good agreement with those obtained by other independent methods as well as with the literature data (see further). Therefore, a more probable reason for the low activation energy E_a observed seems to be not sufficiently developed structure (lattice) of the films during their deposition process.

As it was shown in the papers of A. Rivera et al. [19] and K. L. Ngai et al. [21, 22], the low-temperature conduction mechanism of YSZ (as well as other ionic conductors) may be influenced by the lattice via establishing of the correlations for the ion motion. Oxygen vacancies are known to be associated into the defect complexes (centers), as it was shown also in the present study, and since not all oxygen sites are equivalent, it may enhance the correlations in the low-temperature diffusion process (e.g. [22]). The studies of correlations effects in the conductivity relaxation have shown [19, 20, 21], that a system without interactions (e.g. an isolated molecule in a dilute solution) usually relaxes exponentially. However, when such systems are densely packed and interacting with each other, the relaxation may proceed in various ways and exhibit many interesting properties, such as, a lower activation energy, the value of which depends on the correlation strength.

High-k metal oxides such as ZrO_2 , HfO_2 and Pr_2O_3 are the promising candidates for the gate dielectrics in metal-oxide-semiconductor (MOS) devices [23, 24, 25, 26, 27]. The relative effective permittivity ϵ_r of the YSZ thin films investigated in the present study was obtained using the usual formula $\epsilon_r = Ct / \epsilon_0 S$ by three independent ways directly from the corresponding:

- bulk parallel capacitance, C_P , measured at room temperature and frequency of 1 MHz [28]
- capacitance, C_{imp} of the bulk semicircle maximum in the impedance diagram (modelled by parallel combination of resistor and capacitor and using LSQ technique),
- accumulation capacitance, C_{acc} determined from C-V curves of MIS structures [28],

where t , S , ϵ_0 are the film thickness, gate area and permittivity of free space (8.845×10^{-14} F cm^{-1}), respectively. The capacitances and the corresponding relative permittivities obtained can be found in Tab. 2. The ϵ_r values are in a good agreement with the literature data [28, 29] and confirm YSZ as a high-dielectric constant material also in the form of a thin film.

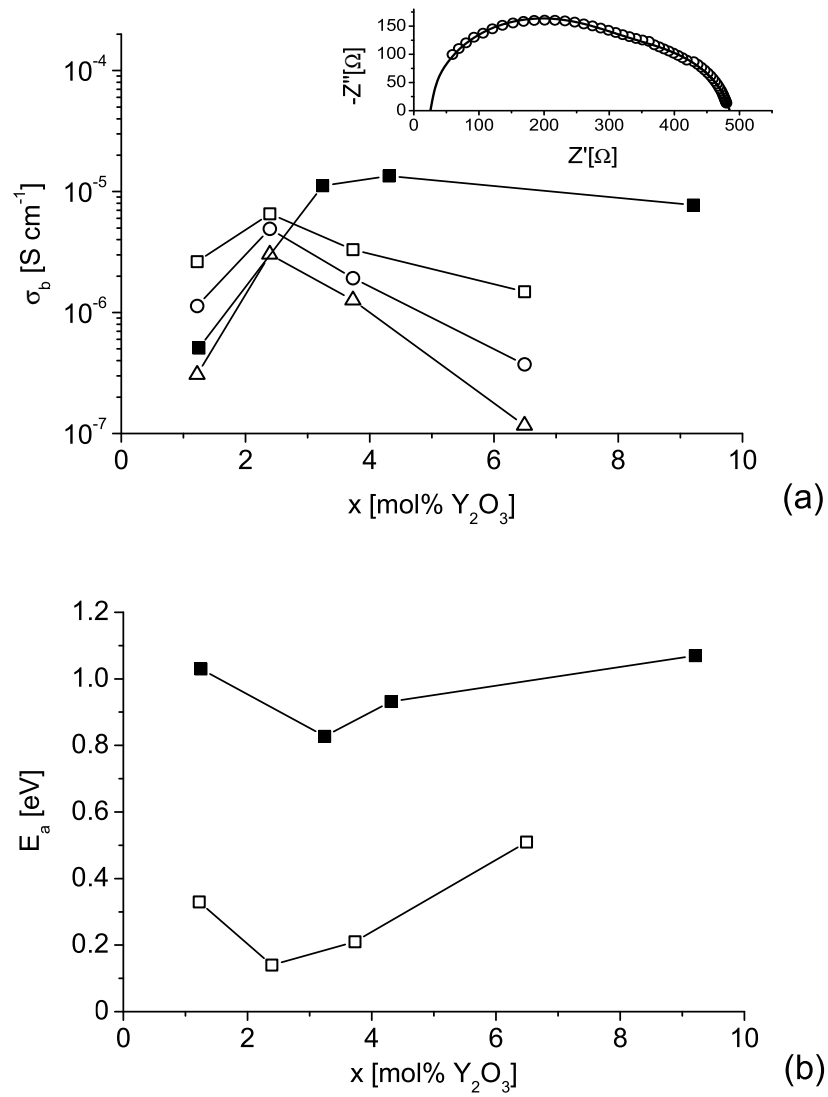


Fig. 2. (a) Isothermal dependences of the bulk conductivity σ_b of YSZ thin films on the amount of Y_2O_3 and taken at the temperatures (with the inset of impedance diagram for $\text{ZrO}_2 + 2.39 \text{ mol\% } \text{Y}_2\text{O}_3$ at 261°C): (Δ) 201°C , (\circ) 261°C , (\square) 323°C and (\blacksquare) YSZ crystalline samples measured at 320°C [7]; (b) Influence of the amount of Y_2O_3 on the activation energy E_a of YSZ: (\square) thin films and (\blacksquare) crystalline samples [7]; both in the low-temperature region and measured in air.

Tab. 2. Capacitances C_p , C_{imp} , C_{acc} and the relative permittivities ε_r of $ZrO_2 + x \cdot Y_2O_3$ mol% thin films deposited by e-beam evaporation at 750°C on the Si (111) substrate.

x [mol% Y_2O_3]	C_p [pF]	$\varepsilon_r (C_p)$	C_{imp} [pF]	$\varepsilon_r (C_{imp})$	C_{acc} [pF]	$\varepsilon_r (C_{acc})$
1.22	599	23	635	26	288	29
2.39	985	26	943	25	383	26
3.73	1479	19	1370	21	700	24
6.49	1113	17	1208	18	450	17

3.3 Microhardness tests.

There is a significant interest in zirconia ceramic (polycrystalline) films as hard coatings to improve the wear and corrosion resistance of materials [30, 31, 32], including thermal barrier coatings [33, 34, 35] and optical coatings [36].

The hardness of thin dielectric films applicable as surface coatings is an important mechanical characteristic. However, due to the small thickness, the measured hardness is usually influenced by the substrate. In order to distinguish the properties of the film from those of the substrate, it is possible to reduce the load so that the indentation is small enough not to be influenced by the substrate. However, the problem for most of the materials is that the hardness cannot be defined for very small indentations [37, 38]. Another approach could be to separate the film hardness from the substrate. Several hardness models have been proposed for this aim [39, 40, 41]. In the present study, the room temperature Vickers microhardness value H_f of a thin ductile film was estimated using the Jonsson-Hogmark model [39]. This method is based on the calculation of the relative contributions of the substrate and film to the effective microhardness. The effective microhardness is expressed as the weighted average of the substrate hardness and the film hardness according to the relation

$$H_f = H_s + \frac{H_c - H_s}{2C \frac{t}{D} - C \left(\frac{t}{D}\right)^2}, \quad (1)$$

where H_f is the microhardness of the ductile film, H_s is the microhardness of the substrate, H_c is the microhardness of the whole cell (i.e. the thin ductile film together with the substrate), t is the thickness of thin ductile film and D is the depth of indentation (equal to the 1/7 of the measured indentation diagonal length). The constant C is determined by the geometry of indentation (the top angle of indenter) and the mechanical properties of the system (in our case the film is harder than the substrate). Microhardness data as a function of yttria content are presented in Fig. 3. As it can be seen, the value of microhardness H_f increases with increasing amount of yttria in the sample in agreement with the increasing structural ordering. Neither load dependence (in the investigated region), nor cracking around the indent (impression) were observed. The present microhardness data obtained under the given conditions (indenter, load and phase / chemical composition) are in a good agreement with the corresponding literature data (e.g. [42]). However, these values obtained, in the comparison with that for the corresponding crystalline systems, are lower (Fig. 3). In spite of it, YSZ in the form of thin film with a well developed structure seems to be the material suitable for a protective layer for metals.

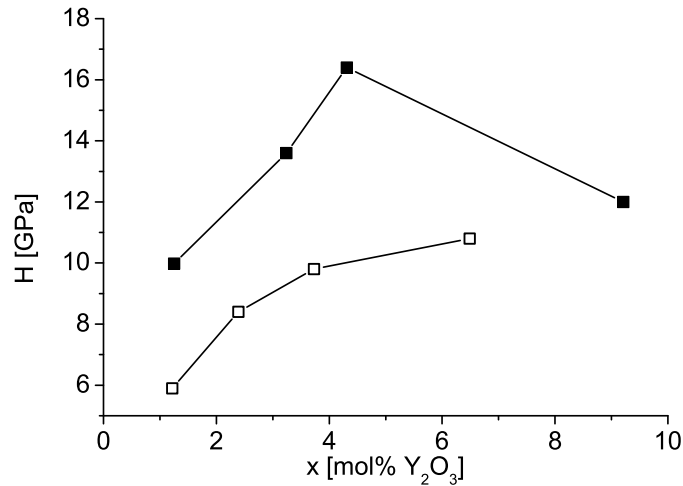


Fig. 3. Room temperature Vickers microhardness value H of YSZ as a function of Y_2O_3 amount measured at the load of 1.1 N: (□) thin films and the corresponding (■) crystalline samples [7]

3.4 Refractive index

Zirconia is of interest also for optical devices because of its favourable properties, particularly the high refractive index, which is possible to obtain, as shown from the reflectance measurements (e. g. [43]).

Reflectance spectra of the YSZ thin films under investigation are qualitatively very similar (Fig. 4) with an exception of the film with 1.22 mol % Y_2O_3 , the data of which could not be reliably evaluated due to a large absorption and consequently a low reflectance. As an example, the reflectance spectrum of the zirconia doped with 2.39 mol% Y_2O_3 with the inset showing the fitting curve are presented in Fig. 5. The measured reflectance spectra have shown that the films are not absorbing in the investigated spectral region (400 – 800 nm). However, they were found to be inhomogeneous along their thickness. If a linear change of the refractive index along the film thickness is assumed, we can obtain the values of normal refractive index, n , using the well-known Cauchy equations for the refractive indices at the air-film and the film-silicon interfaces. Such values of normal refractive index, n , obtained at the wavelength $\lambda = 550$ nm from fitting the reflectance data by means of the Marquard's non-linear least-square fitting procedure are shown in Table 3.

Table 3 contains also the refractive index of undoped ZrO_2 film obtained by the other authors under approximately the same conditions (substrate temperature T_S , λ), deposited however, by the sputtering method [44]. The refractive index at the wavelength of 550 nm was found to slightly decrease with an increase of Y_2O_3 amount in zirconia, namely from 2.20 for 2.39 mol % Y_2O_3 to 1.96 for 6.49 mol % Y_2O_3 . This behaviour is in a good agreement with the literature

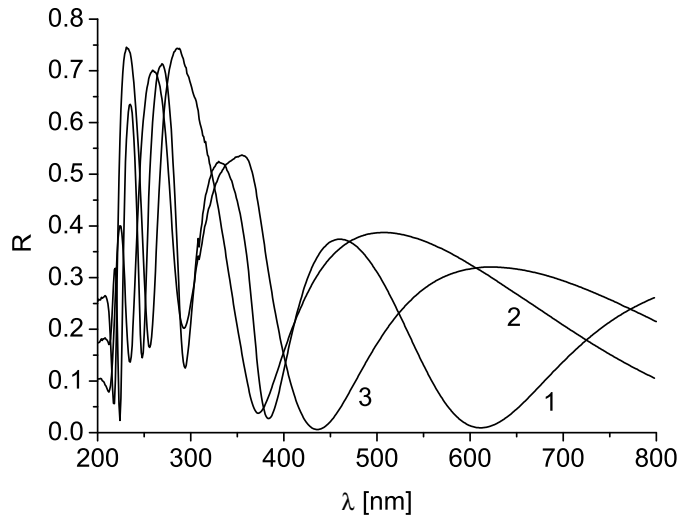


Fig. 4. Reflectance spectra of YSZ thin films as a function of wavelength λ : (1) 2.39 mol% Y_2O_3 , (2) 3.73 mol% Y_2O_3 and (3) 6.49 mol% Y_2O_3 measured in air at room temperature.

data [43, 45] and could be attributed to the change of the crystal structure. Because we have not investigated the optical properties of the crystalline systems [7], the corresponding comparison was performed with the literature data. As an example, the refractive indices n for the crystalline cubic YSZ sample are ranging between 2.159 – 2.198 at room temperature and the wavelength of 632.8 nm in dependence on the yttria content of 10 – 20 wt. % [46]. It means that the present data for the investigated cubic YSZ thin films are in a good mutual agreement with that for the crystalline ones.

Tab. 3. Refractive indices (n) of the YSZ thin films deposited by e-beam evaporation at 750°C on the Si (111) substrate and measured at the wavelength $\lambda = 550$ nm.

x [mol% Y_2O_3]	n
0.00	~ 2.22
1.22	-
2.39	2.20
3.73	2.14
6.49	1.96

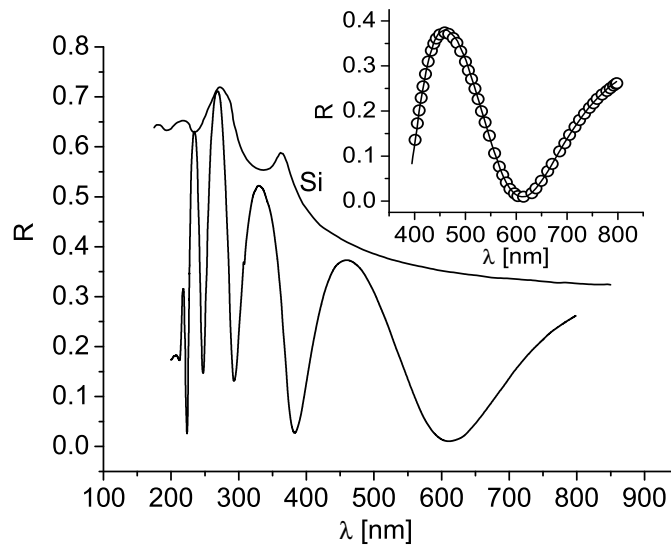


Fig. 5. Reflectance spectrum of zirconia thin film doped with 2.39 mol% Y_2O_3 on Si (111) substrate with the inset showing the fitting curve.

4 Summary

The investigation has provided the following interesting results :

- The structure of all oxide film configurations under investigation was found to be polycrystalline, the rough crystallite sizes being 20.3 nm for the sample with 6.49 mol% Y_2O_3 and 18 nm for the sample with 3.73 mol% Y_2O_3 . Rietveld analysis of diffraction patterns discovered at least two structurally different phases, one cubic (fcc) phase with an increasing degree of perfection as the Y_2O_3 content increases and the other one which may be presumably a highly distorted form of some regular phase in the samples with 3.73 and 6.49 mol% Y_2O_3 . No satisfactory phase indentation could be done at the samples with 1.22 and 2.39 mol% Y_2O_3 .
- The bulk conductivity σ_b and activation energy E_a as the functions of yttria content indicate the presence of isolated oxygen vacancies as well as the associated point defects, the conductivity maximum and the minimum of activation energy at ~ 2.39 mol% Y_2O_3 .
- The relative dielectric permittivities $\epsilon_r = 17 - 26$ obtained by three independent ways confirmed YSZ as a high-dielectric constant material also in the form of thin film.

- The measured microhardness data, $H = 5.9 - 10.8$ GPa, evaluated according to the Jonsson-Hogmark hardness model, have increased with the increasing perfection of the fcc phase and show YSZ as a material suitable for a protective layer for metals.
- A relatively high refractive index, $n = 2.20 - 1.96$, can be attributed to the change of crystal structure and utilized in the optical devices.
- In spite of some imperfections in the structural development of the investigated films during their deposition process, which influence some of the investigated physical properties, it can be concluded that in the case of sufficiently well developed structures, YSZ as a dielectric film is a promising candidate for many interesting applications.

Acknowledgement: The work was supported by the research grants No. 2 / 4105/04, 2 / 3149/23, 2 / 4100 /04, 2 / 2068 / 22 of the Slovak Grant Agency and No. 416072 of the Czech Grant Agency.

References

- [1] H. S. Isaacs: *Adv. Ceramics* **3** (1981) 406
- [2] G. Velasco: *Solid State Ionics* **9/10** (1983) 783
- [3] S. Chandra: *Superionics Solids*, North-Holland, Amsterdam 1981
- [4] J. Han, Y. Zeng, G. Xomeritakis, Y. S. Lin: *Solid State Ionics* **98** (1997) 63
- [5] K. Yasuda, S. Suenaga, H. Inagaki, Y. Goto, H. Takeda: *J. Mater. Sci.* **35** (2000) 317
- [6] T. Inoue, Y. Yamamoto, S. Koyma, B. Suzuki, Y. Ueda: *J. Appl. Phys. Lett.* **56** (1990) 1332
- [7] M. Hartmanová, J. Schneider, V. Navrátil, K. Kundracik, H. Schulz, E. E. Lomonova: *Solid State Ionics* **136 - 137** (2000) 107
- [8] S. Chromik, B. Wuyts, I. Vávra, A. Rosová, F. Hanic, S. Beňačka, Y. Bruynseraede: *Physica C* **226** (1994) 153
- [9] J. H. Scofield: *J. Electron Spectrosc. Relat. Phenom.* **8** (1976) 129
- [10] Tanuma, C. J. Powell, D. R. Penn: *Surf. Interface Anal.* **20** (1993) 77
- [11] P. Jiříček: *Czech. J. Phys.* **44** (1994) 261
- [12] W. H. Kohl: *Handbook of materials and techniques for vacuum devices* Reinhold Publishing Co., New York 1967
- [13] A. Roth: *Vacuum Technology* Elsevier, Amsterdam 1990
- [14] H. R. Philipp, E. A. Taft: *Phys. Rev.* **120** (1960) 37
- [15] A. D. Krawitz: *Introduction to Diffraction in Materials Science and Engineering* John Willey & Sons, New York 2001
- [16] F. Kundracik, M. Hartmanová, J. Müllerová, M. Jergel, I. Kostič, R. Tucoulou: *Mater. Sci. & Engn. B* **84** (2001) 167
- [17] F. Kundracik, M. Hartmanová: *Ionics* **7** (2001) 1
- [18] E. Wanzenberg, F. Tietz, D. Kek, P. Panjan, D. Stover: *Solid State Ionics* **164** (2003) 121
- [19] A. Rivera, J. Santamaria, C. Leon: *Appl. Phys. Letters* **78** (2001) 610
- [20] K. Y. Tsang, K. L. Ngai: *Phys. Rev. E* **54** (1996) R3067
- [21] K. L. Ngai, K. Y. Tsang: *Phys. Rev. E* **60** (1999) 4511

- [22] J. P. Goff, W. Hayes, S. Hull, M. T. Hutchings, K. N. Clausen: *Phys. Rev. B* **59** (1999) 14202
- [23] J. Kwo, M. Hong, A. R. Kortan, K. T. Queeney, Y. J. Chabal, J. P. Mannaerts, T. Boone, J. J. Krajewski, A. M. Sergent, J. M. Rosamilia: *J. Appl. Phys. Lett.* **77** (2000) 130
- [24] K. J. Hubbard, D. G. Schlom: *J. Mater. Res.* **11** (1996) 2757
- [25] R. Sharma, A. C. Rastogi: *J. Appl. Phys.* **76** (1994) 4215
- [26] L. Manchanda, M. Gurvitch: *IEEE Electron Device Lett.* **9** (1988) 180
- [27] S. K. Tik, G. C. Smith: *IEEE Electron Device Lett.* **9** (1988) 180
- [28] M. Hartmanová, K. Gmucová, I. Thurzo: *Solid State Ionics* **130** (2000) 105
- [29] M. Croset, J. P. Scnell, G. Velasco, A. J. Siejka: *J. Appl. Phys.* **48** (1977) 775
- [30] M. Anast, J. M. Bell, T. J. Brell, B. Ben-Nissan: *J. Mater.Sci. Lett.* **11** (1992) 1483
- [31] K. Izumi, M. Murakami, T. Deguchi, A. Morita: *J. Amer. Ceram. Soc.* **72** (1989) 1465
- [32] A. S. Kao, C. Hwang: *J. Vacuum Technol. A* **8** (1990) 3289
- [33] M. Shane, M. L. Mecartney: *J. Mater.Sci.* **25** (1990) 1537
- [34] A. S. James, A. Matthews: *Surf. Coating Technol.* **41** (1990) 305
- [35] J. R. Brandon, R. Taylor: *Surf. Coating Technol.* **39** (1989) 143
- [36] M. Ghanashyam Krishna, K. Narasimha Rao, S. Mohan: *Thin Solid Films* **193/194** (1990) 690
- [37] M. Nishibori, K. Kinoshita: *Thin Solid Films* **48** (1978) 325
- [38] M. Tazaki, M. Nishibori, K. Kinoshita: *Thin Solid Films* **51** (1978) 13
- [39] B. Jonsson, S. Hogmark: *Thin Solid Films* **114** (1984) 257
- [40] P. J. Burnett, T. F. Page: *J. Mater. Sci.* **19** (1984) 845
- [41] J. L. He, W. Z. Li, H. D. Li: *J. Appl. Phys. Lett.* **69** (1996) 1402
- [42] P. S. Alexopoulos, T. C. O'Sullivan: *Annu. Rev. Sci.* **20** (1990) 391
- [43] W.-Ch. Liu, D. Wu, A.-D. Li, H.-Q. Ling, Y.-F. Tang, N.-B. Ming: *Appl. Surf. Sci.* **191** (2002) 181
- [44] H. Uyama, N. Oka, I. Ono, O. Matsumoto: *Denki Kagaku* **58** (1990) 564
- [45] M. Boulouz, A. Boulouz, A. Giani, A. Boyer: *Thin Solid Films* **323** (1998) 85
- [46] J.G. Cai, E. Anastassakis: *Phys. Rev.B* **51** (1995) 6821